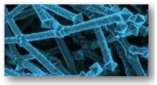
Materiales

Revista Mexicana de Ingeniería Química
Vol. 14, No. 2 (2015) 481-487

THERMAL PARAMETERS STUDY OF BIODIESEL CONTAINING Au NANOPARTICLES USING PHOTOTHERMAL TECHNIQUES

ESTUDIO DE PARÁMETROS TÉRMICOS DE BIODIESEL CONTENIENDO NANOPARTÍCULAS DE Au USANDO TÉCNICAS FOTOTÉRMICAS

J.L. Jiménez-Pérez[1]*, G. López-Gamboa[1,2], A. Cruz-Orea[3] and Z.N. Correa-Pacheco[4]

[1]*UPIITA-IPN, Avenida Instituto Politécnico Nacional, No. 2580, C.P. 07340, México D.F., México.*
[2]*UPVT km 5.7 Carretera Almoloya de Juárez, Santiaguito Tlalcilalcali, C.P. 50904 Edo. México, México.*
[3]*Departamento de Física, CINVESTAV-IPN, Av. Instituto Politécnico Nacional No. 2508, C.P. 07360 México, D.F., México.*
[4]*IPN-Centro de Desarrollo de Productos Bióticos. Carretera Yautepec-Jojutla, km 6.8, Morelos, México CP 62730.*

Received November 9, 2014; Accepted April 27, 2015

Abstract

Thermal parameters of biodiesel containing Au nanoparticles was characterized by thermal lens technique (TL) and inverse photopyroelectric (IPPE) technique. In the case of the TL spectrometry technique, two lasers in the mismatched mode experimental configuration were used in order to obtain the thermal diffusivity (D) of the biodiesel. On the other hand, the sample thermal effusivity (e) was obtained by using the IPPE technique where the temperature variation of the sample, exposed to modulated radiation, is measured with a pyroelectric sensor. In this technique a He-Ne laser was used as the excitation source and was operated at 632 nm with an output power of 120 mW. From the obtained thermal-diffusivity (D) and thermal effusivity (e) values, the thermal conductivity (k) was calculated from the relationship $e = k/\sqrt{D}$. The obtained thermal parameters were compared with the values of the thermal parameters of literature. Measurements of particle size and absorption were determined by complementary techniques such as transmission electron microscopy (TEM) and photoacoustic (PA) spectroscopy, respectively. Our work has applications as high functioning heat transfer fluids in automotive electronic cooling systems and in micro-channel heat sinks (Wen *et al*., 2006).

Keywords: Au nanoparticles, thermal lens, thermal diffusivity, thermal effusivity, thermal conductivity.

Resumen

Los parámetros térmicos del biodiesel conteniendo nanopartículas de Au fueron caracterizados por las técnicas de lente térmica (TL) y técnica fotopiroeléctrica inversa (IPPE). En el caso de TL, en la configuración experimental en el modo desacoplado de dos láseres fue usado con la finalidad de obtener la difusividad térmica (D) del biodiesel. Por otra parte, la efusividad térmica de la muestra (e) fue obtenida mediante el uso de la técnica IPPE donde la variación de la temperatura de la muestra, expuesta a la luz modulada, es medida con un sensor piroeléctrico. En esta técnica un láser de He-Ne fue usado como fuente de excitación y fue operado a 632 nm con una potencia de salida de 120 mW. De los valores de la difusividad térmica (D) y la efusividad térmica (e), la conductividad térmica (k) fue calculada de la relación $e = k/\sqrt{D}$. Los parámetros térmicos obtenidos fueron comparados con los valores de los parámetros térmicos de la literatura. La mediciones del tamaño de partícula y de la absorción fueron determinados por técnicas complementarias tales como TEM y espectroscopia fotoacústica (PA), respectivamente. Nuestro trabajo tiene aplicaciones en fluidos de alto rendimiento y en microcanales como disipadores de calor (Wen *et al*., 2006).

Palabras clave: nanopartículas de Au, lente térmica, difusividad térmica, efusividad térmica, conductividad térmica.

* *Corresponding author. E-mail*: : jimenezp@fis.cinvestav.mx
Tel. 52-55-5729-6300 ext. 56911

1 Introduction

The thermal properties of biodiesel have been subject of great study. The poor heat transfer properties of conventional fluid such as mineral oil, ethylene glycol and water are a big challenge for heating and cooling system in many industrial processes and applications such as high functioning heating transfer fluids in automotive, electronic cooling, and in microchannel heat sinks. In order to solve this poor heat transfer of fluids, conductive materials such as gold nanoparticles have been employed to increase the amount of thermal diffusivity of the liquids (Zamiri *et al*., 2012).

The study of different thermal properties of biodiesel, such as thermal conductivity, diffusivity, and effusivity, is a major interest among the thermo physical properties, because of their application mainly in heat transfer processes (González *et al*., 2014; Kourentzi *et al*., 2014; Vázquez-Nava *et al*., 2007).

The TL method can be successfully employed for the determination of thermal diffusivity, especially in nanofluids. TL is produced, when a light energy is converted into heat, generating a transient temperature profile. This increase in temperature changes the refraction index, forming a thermal lens. These effects cause focusing or defocusing of the light beam (depending upon the sign of the change of the refraction index with temperature) (Pedreira *et al*., 2003). By monitoring this transient thermal lens, the thermal diffusivity can be determined.

The inverse photopryroelectric (IPPE) method is well known for investigation thermal parameters of some materials such as crystals (Dadarlat *et al*., 1993), tomato paste (Bicanic *et al*., 2004), liquids (Caerels *et al*., 1998), fatty acids and triglycerides (Menon *et al*., 2009), among others. Physical properties of biodiesel are subject of intensive research both in industry and academic (Ventura *et al*., 2013; George 2002).

In the IPPE method the laser impinges on the surface of the pyroelectric sensor which back is in thermal contact with the sample. The temperature oscillations are detected by the pyroelectric transducer and the amplified by the lock-in. By modulation the light source using a mechanical chopper at a certain frequency, the thermal oscillation is also modulated. The IPPE configuration was used in this study because any possible detection problem related to the optical properties of the sample (transparency, thermal reflectance) is avoided.

The exact determination of thermal diffusivity by TL of the biodiesel would be complementary to the thermal effusivity obtained by IPPE. By measuring the thermal effusivity, the material thermal impedance or the ability of the sample to exchange the heat with its surroundings can be demonstrated (Mota *et al*., 2008; El-Brolossy *et al*., 2010).

The two dynamic thermal parameters, that is, thermal diffusivity D and effusivity e is connected with other thermal parameters, that is, thermal conductivity k and volumetric specific heat c_p by $D = k/\rho c_p$ and $e = (k\rho c_p)^{1/2}$ where ρ is the density of sample.

In this paper we report the use of TL and IPPE techniques for measuring the thermal diffusivity and effusivity of biodiesel with Au nanoparticles, respectively. The thermal diffusivity, thermal effusivity and thermal conductivity values will be obtained in the present work.

2 Experimental

Biodiesel, a vegetable oil consisting of long-chain methyl esters from waste oils, is used in several industrial applications, as a key raw-material for the production of several commodities like paints, polymers, lubricants, fuel, etc. Biodiesel oils are a mixture of triglycerides, predominantly derived from an unsaturated and hydroxilated fatty acid, called ricinoleic acid. In view of studying nanoparticle induced heat transport enhancement, Au nanoparticles were prepared by the reduction of Gold (III) chloride trihydrate using hydrazine as a reducing agent in a microemulsion (reverse micelle) system containing isooctane, deionized water, dioctylsulfosuccinate sodium salt as surfactant and dodecanethiol as co-surfactant. Next, the Au nanoparticles were mixed into biodiesel, purchased from Biofuels of Mexico (biodiesel C 4), to obtain six sample materials with different concentrations of Au nanoparticles (1/5, 3/5, 5/5, 7/5, 8/5, and 10/5 mg/ml). Measurements of particle size and absorption were determined by complementary techniques such as transmission electron microscopy (TEM) and PA spectroscopy, respectively.

The TL effect is caused by the deposition of heat via non-radiative decay processes after the laser beam with Gaussian profile has been absorbed by the sample. In this situation, a transverse temperature profile, $\Delta T(r,t)$ in the sample, is established. The temporal evolution $\Delta T(r,t)$ is scaled according to characteristic time constant:

$$t_c = \omega_e^2/4D \tag{1}$$

where ω_e is the excitation laser beam radius at the sample and D is the thermal diffusivity (Jiménez *et al.*, 2010). Owing to $\Delta T(r,t)$, a temperature coefficient of the optical path length change, $ds/dT = dn/dT$ (for liquids), is generated, creating a lens-like optical element: the so-called TL effect. The propagation of a probe laser beam through this TL, results in a variation of its on-axis intensity $I(t)$, which can be calculated using diffraction integral theory. In transient regime, an analytical expression can be obtained for the probe beam intensity, $I(t)$ (Gutiérrez *et al.*, 2007; Shen *et al.*, 1992):

$$\frac{I(t)}{I(0)} = \left[1 - \frac{\theta}{2}\tan^{-1}\left(\frac{2mV}{\left[(1+2m)^2+V^2\right]\frac{t_c}{2t}+1+2m+V^2}\right)\right]^2 \quad (2)$$

where:

$$m = \left(\frac{\omega_{1p}}{\omega_e}\right)^2; \quad V = \frac{Z_1}{Z_c}; \quad \theta = -\frac{P_e A_e l_0}{k\lambda_p}\left(\frac{dn}{dT}\right)_p$$

In Eq.(2), $I(0)$ is the initial value of $I(t)$; θ is the thermally induced phase shift of the probe beam after passing through the sample; Z_c (12.9 cm) is the confocal distance of the probe beam and Z_1 (8.0 cm) is the distance from the probe beam waist to the sample. $\omega_e(\omega_p)$ is the spot size of the excitation (probe) laser beam at the sample; $k(D)$ is the thermal conductivity (diffusivity) of the sample; P_e (40 mW) is the incident power; A_e (cm^{-1}) is the optical absorption coefficient at the excitation beam wavelength λ_e; and dn/dT (K^{-1}) is the temperature dependence of the sample refractive index. The so-called characteristic time t_c of the TL effect's formation, is defined in Eq. (1), where $D = k/\rho c$ with ρ being the density and c is the specific heat of the nanofluid. The experimental value of the beam waist of the excitation laser beam is ω_e =40 μm. Eq. (2) describes the time resolved transient that creates the TL effect. Then by fitting the equation of $I(t)$ (Eq. 2) to the experimental data, as a function of time (t), it is possible to obtain the sample thermal diffusivity D from t_c and θ as adjustable parameters. An excitation laser of Ar^+ is used, at λ= 514 nm, which was focused by a converging lens L_1, and the sample was placed at the focal plane lens. Exposure of the sample to the excitation beam was controlled by means of a shutter, which was connected directly to the trigger of a digital oscilloscope. A second He-Ne laser probe beam of 4mW was focused with a lens L_2.The probe beam was incident on the sample and carefully centered to pass through the thermal lens to maximize the thermal-lens signal. The schematic diagram of the TL experimental setup is shown in Fig. 1 (Shen *et al.*, 1992).

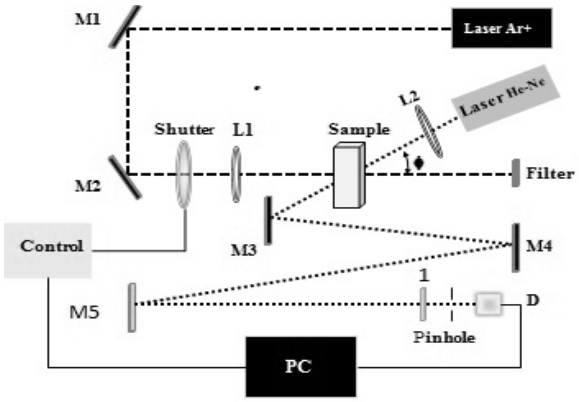

Fig. 1 Schematic diagram of TL experimental setup.

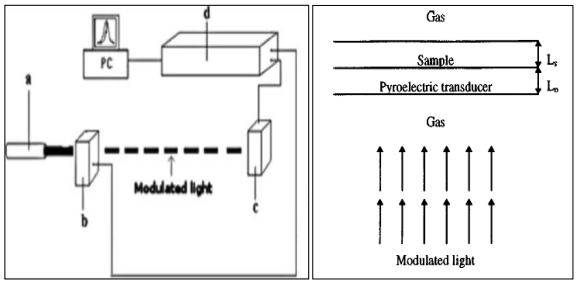

Fig. 2 Experimental setup used to obtain the IPPE signal: a) laser, b) acousto-optic modulator, c) pyroelectric detector, d) lock-in amplifier. On the right, the open photoacoustic cell is shown (detail of c).

On the other hand, in a typical IPEE configuration, the sample is in contact with the back of the detector. A modulated light beam impinges in the PVDF pyroelectric detector and the emitted signal is a function of the light modulation frequency. The thermal effusivity is obtained by fitting the theoretical equations to the experimental data. The experimental setup is shown in Fig. 2.

For the IPPE geometry, when thermally thick sample is assumed, the theoretical expression used to fit the experimental data is shown in Eq. (3) (Caerels *et al.*, 1998; Cervantes-Espinosa *et al.*, 2012):

$$\theta(\omega) = \frac{(1-e^{q_p l_p})(1+b)+(e^{-q_p l_p}-1)(1-b)}{(g-1)e^{-q_p l_p}(1-b)+(1+g)e^{q_p l_p}(1+b)} \quad (3)$$

Where $\theta(\omega)$ is proportional to the output signal of the pyroelectric detector (PE), l_p is the detector thickness, $\omega = 2\pi f$, $q_p = (j2\pi f/\alpha_p)^{1/2}$, $b = e_s/e_p$, and $g = e_g/e_p$ with e_s, e_g, and e_p being the thermal effusivity for

sample, air, and PE, respectively. Thereby, the fitting parameter b is obtained and e_s can be evaluated by using Eq. 3 where e_g, l_p, and e_p are well known (Cruz-Orea *et al*., 2013).

3 Results and discussions

The PA optical absorption spectra of 1/5, 7/5, 8/5 and 10/5 gold nanoparticles with biodiesel are shown in Fig. 3 (a). Through the absorption spectrum, it can be seen a broad absorption band between 300-600 nm with a peak at 350 nm. Also gold nanoparticle solutions showed an absorption band at 523 nm (corresponding to incident laser λ = 514 nm). Fig. 3 (b) shows a TEM image of the gold nanoparticles, which mean diameter, was 9 nm. The particles have a spherical shape and are well dispersed (not agglomerates are observed).

Fig. 4a) and Fig. 4b) show a typical transient thermal lens signal evolution for biodiesel with an Au nanoparticle concentration of 1/5 and 5/5 mg/ml, respectively. The experimental TL signal is represented by open circles, while the solid line corresponds to the best fitting of Eq. (2) to experimental data, with θ = 9.50±0.03 $\times10^{-2}$ and t_c= 22.9±0.4 $\times10^{-4}$ s for concentration 1/5 and θ = 8.33±0.04 $\times10^{-2}$ and t_c= 21.4±0.3 $\times10^{-4}$ s for concentration 5/5, as adjustable parameters. Related to diffusivity, for concentration 1/5 value was D = 17.46±0.30 $\times10^{-4}$ cm$^2\cdot$ s^{-1} and for concentration 5/5 value was D = 18.69±0.26 $\times10^{-4}$ cm$^2\cdot$ s^{-1}, as best fitting parameter values. In a similar way, from the best fitting of Eq. (2) to the experimental data, the thermal diffusivities of the other nanofluid samples were obtained at room temperature: D = (17.85±0.31) $\times10^{-4}$ cm$^2\cdot$ s^{-1}, D = (19.60±0.28) $\times10^{-4}$ cm$^2\cdot$ s^{-1}, D = (21.39±0.34) $\times10^{-4}$ cm$^2\cdot$ s^{-1} and D = (22.59±0.38) $\times10^{-4}$ cm$^2\cdot$ s^{-1} for samples with Au nanoparticle concentrations 3/5, 7/5, 8/5, and 10/5 mg/ml, respectively. The thermal diffusivity values obtained for biodiesel with gold nanoparticles are (slightly) higher than the pure biodiesel, 16.9 ± 0.4 $\times10^{-4}$ cm$^2\cdot$ s^{-1}. The reported value in the literature for biodiesel is 14.04 $\times10^{-4}$ cm$^2\cdot$ s^{-1} and for diesel is 17.15 $\times10^{-4}$ cm$^2\cdot$ s^{-1} (Božiková *et al*., 2013; Guimarães *et al*., 2012).

Thermal effusivity was obtained by using the IPPE configuration. Fig. 5 shows the signal phase (Fig. 5a) and amplitude (Fig. 5b) as a function of the incident beam modulated frequency for the biodiesel for concentration de 8/5. The solid line corresponds to the best fit of Eq. (3) with the normalized phase and amplitude signal. From the best fitting of the amplitude of Eq. (3) with the IPPE normalized amplitude signal data. Thermal effusivity value of e_s = 598.9 ± 5.3 W s$^{1/2}$ m^{-2} K^{-1} was obtained. In a similar way, from the best fitting of Eq. (3) to the experimental data, the thermal effusivities of the other nanofluid samples were obtained: e = (551.20 ± 5.3) W s$^{1/2}$ m^{-2} K^{-1}, e = (557.32 ± 5.3) W s$^{1/2}$ m^{-2} K^{-1}, e = (558.00 ± 3.2) W s$^{1/2}$ m^{-2} K^{-1} , e = (588.9 ± 5.3) W s$^{1/2}$ m^{-2} K^{-1}, e = (598.9 ± 5.3) W s$^{1/2}$ m^{-2} K^{-1} and e = (600.42 ± 5.3) W s$^{1/2}$ m^{-2} K^{-1} for samples with Au nanoparticle concentrations 1/5, 3/5, 5/5, 7/5 and 10/5 mg/ml, respectively.

By using the obtained values of thermal diffusivity (D) and thermal effusivity (e_s), the thermal conductivity (k) was calculated from relationship ($k = e_s\sqrt{D}$.). The thermal conductivity for biodiesel (8/5) was calculated to be 27.69 ± 0.3$\times10^{-2}$ W/mK.

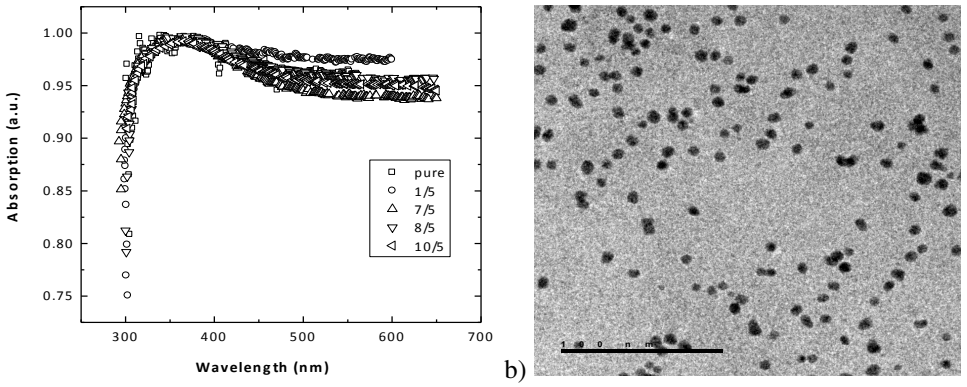

Fig. 3 (a) The PA optical absorption spectra of 1/5, 7/5, 8/5 and 10/5 gold nanoparticles with biodiesel; 3 (b) TEM image of the gold nanoparticles, which mean diameter was 9 nm.

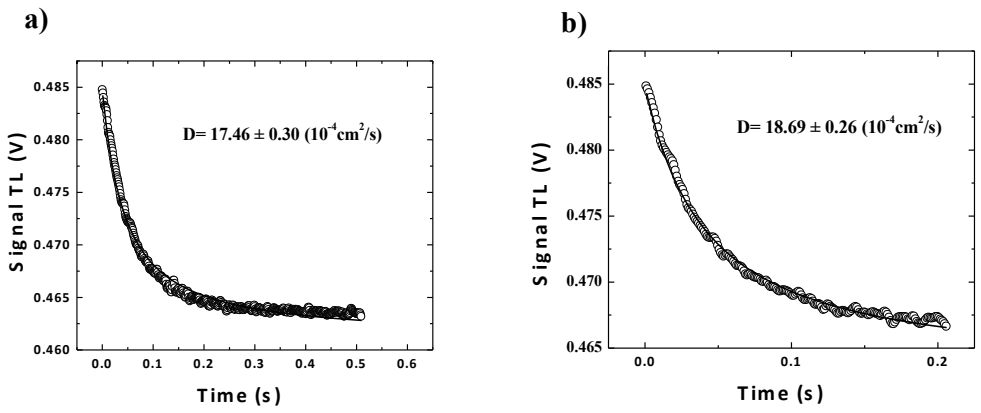

Fig. 4 The normalized TL time evolution signal for concentrations: a) (1/5) and b) (5/5).

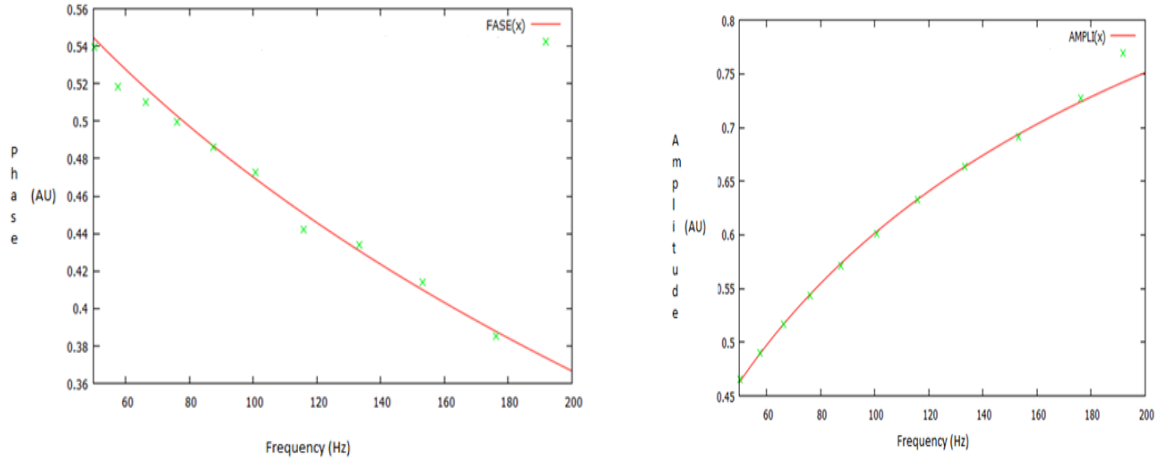

Fig. 5 Thermal effusivity plot: a) (phase vs. frequency) and b) (amplitude vs. frequency) for concentration (8/5).

Table 1.Values of thermal diffusivity, thermal effusivity and thermal conductivity for the different concentrations.

Sample(mg/ml)	D(10^{-8}m^2/s)	e(Ws$^{1/2}$/m^2 K)	k(10^{-2}W/mK)
Pure	16.94±0.4	543.76±4.4	22.35±0.3
1/5	17.46±0.3	551.20±5.3	23.03±0.3
3/5	17.85±0.3	557.32±5.3	23.54±0.3
5/5	18.69±0.3	558.00±3.2	24.12±0.2
7/5	19.60±0.3	588.9±5.3	26.07±0.3
8/5	21.39±0.3	598.9±5.3	27.69±0.3
10/5	22.59±0.4	600.42±5.3	28.54±0.3

The reported value of thermal effusivity in the literature for biodiesel (castor oil) is 544 ± 0.08W s$^{1/2}$ m^{-2} K^{-1}(Castro *et al.*, 2005). This value of thermal effusivity is near to the obtained value for biodiesel (e = 543.76 ± 4.4W s$^{1/2}$ m^{-2} K^{-1}, shown in table 1).

In Table 1 all data of D, e_s, k and ρc are summarized and the values found in the literature are also provided for comparison.

In order to compare the obtained data with some reported values, thermal properties for a sample similar to our biodiesel was found in the literature with a thermal conductivity of k = 0.190 (W/ m K) [17]. This value of conductivity is near to the obtained value for biodiesel (k = 0. 2 ± 0.3W/mK) which supports our

results.

On the other hand, the increment in the thermal conductivity ranges from 5 % (minimum) to 28% (maximum) for the different Au nanoparticle concentrations. There is a slight increase in the fluid thermal conductivity with increasing Au nanoparticle concentration.

Conclusions

The thermal diffusivity and thermal effusivity of biodiesel containing Au nanoparticles were measured by TL and IPPE techniques, respectively. From the thermal diffusivity and thermal effusivity values, thermal conductivity was calculated. Results show a 5 % (minimum) to 28 % (maximum) increase in the conductivity of biodiesel. Biodiesel thermal parameter values are reported in this paper for the first time being in the range of typical vegetable oils samples.

Acknowledgments

We thank CONACYT, COFAA-IPN, and SIP-IPN, México for their partial financial support.

Abbreviations

Au	gold
TL	thermal lens
IPPE	inverse photopyroelectric
D	thermal diffusivity
e	thermal effusivity
k	thermal conductivity
PVDF	polyvinylidene fluoride
TEM	transmission electron microscopy
PA	photoacoustic spectroscopy

References

Bicanic, D., Neamtu, C., Manojlović, M., van der Linden, D., Dadarlat, D., Posavec, K., Gijsbertsen, A., Kurtanjek, Ž. (2004) Tomato pastes and their moisture content as determined via the measurements of thermal effusivity by means of infrared photothermal radiometry and inverse photopyroelectric technique. *Acta Chimica Slovenica 51*, 39-46.

Božiková, M., Hlaváč, P. (2013) Thermal conductivity and thermal diffusivity of biodiesel and bioethanol samples. *Acta Technologica Agriculturae 4*, 90-94.

Caerels, J., Glorieux,C., Thoen, J. (1998) Absolute Measurement of Specific Heat Capacity and Thermal Conductivity of Liquids from Different Modes of Operation of a Simple Photopyroelectric Setup. *Review of Scientific Instruments 69*, 2452-2458.

Castro, M.P.P., Andrade, A.A., Franco, R.W.A., Miranda, P.C.M.L., Sthel, M., Vargas, H., Constantino, R., Baesso, M.L. (2005) Thermal properties measurements in biodiesel oils using photothermal techniques. *Chemical Physics Letters 411*, 18-22.

Cervantes-Espinosa, L., Castillo-Alvarado, F., Lara-Hernández, G., Cruz-Orea, A., Mendoza-Álvarez, J., Valcárcel, J., García-Quiroz, A. (2012) Thermal Characterization, Using the Photopyroelectric Technique, of Liquids Used in the Automobile Industry. *International Journal of Thermophysics 33*, 1916-1923.

Cruz-Orea, A., Sánchez-Sinencio, F., Algatti, M. A., Jiménez-Pérez, J. L., Correa-Pacheco, Z. N., García-Quiroz, A. (2013) Thermal characterization of Diglyme by using photopyroelectric spectroscopy. *Trends in Heat and Mass Transfer 13*, 51-55.

Dadarlat, D., Frandas, A. (1993) Nonlinearluminiscence phenomena in fullerene crystallites. *Applied Physics A 56*, 235-239.

El-Brolossy, T., Ibrahim, S. (2010) Photoacoustic measurement of thermal properties of polystyrene metal oxide composites. *Thermochimica Acta 509*, 46-49.

George, N. (2002) Thermal diffusivity of liquid crystalline polymers measured using open cell photoacoustic technique. *Smart Materials and Structures 11*, 561-564.

González-Brambila, M.M., Montoya de la Fuente, J.A., González-Brambila, O., López Isanza, F. (2014). A heterogeneous biodiesel production kinetic model. *Revista Mexicana de Ingeniería Química 13*, 311-322.

Guimarães, A.O., Machado, F.A.L., da Silva, E.C., Mansanares, A.M. (2012) Investigating thermal properties of biodiesel/diesel mixtures using photopyroelectric technique. *Thermochimica Acta 52*, 125-130.

Gutiérrez Fuentes, R., Sánchez Ramírez, J. F. , Jiménez Pérez, J. L., Pescador Rojas, J. A,.Ramón Gallegos, E., Cruz Orea, A. (2007) Thermal Diffusivity Determination of Protoporphyrin IX Solution Mixed with Gold Metallic Nanoparticles. *International Journal of Thermophysics 28*, 1048-1055.

Jiménez Pérez, J.L., Sánchez Ramírez, J.F., Cruz Orea, A., Gutiérrez Fuentes, R., Cornejo Monrroy, D., López Muñoz, G.A. (2010). Heat transfer enhanced in water containing TiO_2 nanospheres. *Journal of Nano Research 9*, 55-60.

Kourentzi, K., Willson, R.C. (2014). Nanotechnology for medical diagnostics. *Revista Mexicana de Ingeniería Química 13*, 9-18.

Menon, P., Rajesh, R., Glorieux, C. (2009) High accuracy, self-calibrating photopyroelectric device for the absolute determination of thermal conductivity and thermal effusivity of liquids. *Review of Scientific Instruments 80*, 054904.

Mota, L., Toledo, R., Machado, F., Holanda, J., Vargas, H., Faria, R. (2008) Thermal characterization of red clay from the Northern Region of Rio de Janeiro State, Brazil using an open photoacoustic cell, in relation to structural changes on firing. *Applied Clay Science 42*, 168-174.

Pedreira, P.R.B., Hirsch, L., Pereira, J.R.D., Medina, A.N., Bento, A.C., Baesso, M.L.(2003) Temperature dependence of the thermo-optical properties of water determined by thermal lens spectrometry. *Reviews of Scientific Instrumemnts 74*, 808-810.

Shen, J., Lowe, R.D., Snook,R. D. (1992). A model for cw laser induced mode-mismatched dual-beam thermal lens spectrometry. *Chemical Physics 165*, 385-396.

Vázquez-Nava, E., Lawrence, C.J., Isothermal dissolution of a spherical particle with a moving boundary in a flow field. *Revista Mexicana de Ingeniería Química 6*, 157-168.

Ventura, M., Simionatto, E., Andrade. L.H.C., Simionatto, E.L., Riva, D., Lima, S.M. (2013) The use of thermal lens spectroscopy to assess oil-biodiesel blends. *Fuel 103*, 506-511.

Wen, D. S., Ding, W. (2006) Natural convective heat transfer of suspensions of titanium dioxide nanoparticles (Nanofluids). *IEEE Transactions on Nanotechnology 5*, 5220-227.

Zamiri, R. , Azmi, B. Z. , Husin, M. S. , Zamiri, G., Ahangar, H. A., Rizwan, Z. (2012) Thermal diffusivity measurement of copper nanofluid using pulsed laser thermal lens technique. *Journal of the European Optical Society 7*, 12022-1 -5.